

# Separating speed and ability to displace roadblocks during DNA translocation by FtsK

This is an open-access article distributed under the terms of the Creative Commons Attribution License, which permits distribution, and reproduction in any medium, provided the original author and source are credited. This license does not permit commercial exploitation without specific permission.

Estelle Crozat<sup>1</sup>, Adrien Meglio<sup>2</sup>,  
Jean-François Allemand<sup>2</sup>, Claire E Chivers<sup>1</sup>,  
Mark Howarth<sup>1</sup>, Catherine Vénien-Bryan<sup>1</sup>,  
Ian Grainge<sup>1,3</sup> and David J Sherratt<sup>1,\*</sup>

<sup>1</sup>Department of Biochemistry, University of Oxford, Oxford, UK  
and <sup>2</sup>Laboratoire de Physique Statistique et Département de Biologie,  
Ecole Normale Supérieure, UPMC, Paris 06, Université Paris Diderot,  
CNRS, Paris, France

**FtsK translocates dsDNA directionally at >5 kb/s, even under strong forces. *In vivo*, the action of FtsK at the bacterial division septum is required to complete the final stages of chromosome unlinking and segregation. Despite the availability of translocase structures, the mechanism by which ATP hydrolysis is coupled to DNA translocation is not understood. Here, we use covalently linked translocase subunits to gain insight into the DNA translocation mechanism. Covalent trimers of wild-type subunits dimerized efficiently to form hexamers with high translocation activity and an ability to activate XerCD-*dif* chromosome unlinking. Covalent trimers with a catalytic mutation in the central subunit formed hexamers with two mutated subunits that had robust ATPase activity. They showed wild-type translocation velocity in single-molecule experiments, activated translocation-dependent chromosome unlinking, but had an impaired ability to displace either a triplex oligonucleotide, or streptavidin linked to biotin-DNA, during translocation along DNA. This separation of translocation velocity and ability to displace roadblocks is more consistent with a sequential escort mechanism than stochastic, hand-off, or concerted mechanisms.**

The EMBO Journal advance online publication, 8 April 2010;  
doi:10.1038/emboj.2010.29

Subject Categories: genome stability & dynamics

Keywords: *Escherichia coli* chromosome segregation; FtsK  
DNA translocase; molecular motor

## Introduction

FtsK is a highly conserved dsDNA translocase that functions in the final stages of bacterial chromosome unlinking and in coordinating this final stage of chromosome segregation with

cell division (Begg *et al*, 1995; Yu *et al*, 1998; Recchia *et al*, 1999; Aussel *et al*, 2002; Grainge *et al*, 2007). FtsK is tethered to the developing division septum by its membrane-spanning N-terminal domain and targets its activity to any dimeric, catenated or incompletely replicated chromosomes in the G2 phase of the cell cycle (Steiner *et al*, 1999; Dorazi and Dewar, 2000; Aussel *et al*, 2002).

The C-terminal ~500 amino-acid (aa) FtsK translocase is composed of three subdomains:  $\alpha\beta$  constitute the active motor, whereas the  $\gamma$ -subdomain has regulatory functions. The translocase loads FtsK preferentially at specific DNA sequences that are oriented in the bacterial chromosome. In *Escherichia coli*, FtsK Oriented Polar Sequences (KOPS; GGGNAGGG) are the preferred loading sites from where FtsK translocates DNA at ~5 kb/s (Saleh *et al*, 2004; Pease *et al*, 2005; Bigot *et al*, 2006). Finally, the translocation by FtsK stops at XerCD-bound *dif* sites in the replication terminus region, where FtsK activates the final chromosome unlinking by XerCD recombination at *dif* (Graham *et al*, 2010). The  $\gamma$ -regulatory subdomain of FtsK acts in KOPS loading and in the activation of XerCD recombination at *dif*.

The FtsK translocase belongs to the RecA subgroup of the additional strand catalytic glutamate (ASCE) ATPase superfamily that also contain AAA+ (ATPases associated with various cellular activities) enzymes that have multiple biological roles, including translocating along nucleic acids in the 3'–5' direction. In contrast, translocases and helicases that belong to the RecA group (e.g. T7gp4 and DnaB), translocate in the 5'–3' direction in the cases analysed (Singleton *et al*, 2007; Thomsen and Berger, 2009). It, therefore, seems likely that during FtsK dsDNA translocation, the catalytic mechanism uses just one of the two DNA chains and that translocation is 5'–3' with respect to this chain. The nature of the ASCE folds places the ATP-binding pocket of one subunit close to  $\gamma$ -phosphate sensor elements in an adjacent subunit, thereby providing the opportunity for coordinated catalysis and ATP hydrolysis. A crystal structure of the  $\alpha\beta$  motor of *Pseudomonas aeruginosa* FtsK bound to ADP showed a symmetrical hexamer with no obvious loops protruding into the central chain in which ds DNA is normally located (Massey *et al*, 2006). This led to the proposal of a sequential rotary mechanism for translocation, with a rotational resetting after each catalytic step, which was proposed to translocate 2 bp of DNA. Nevertheless, the structure did not provide any evidence for the asymmetry in structures and nucleotide-binding states that one would predict from such a mechanism.

To further address the FtsK translocation mechanism, we have covalently linked the minimal predicted functional translocase, identified by the crystallographic studies, into multimers using a 14 aa flexible linker. This strategy was previously used to study the hexameric ClpX protein-unfolding motor (Martin *et al*, 2005) and the recombination protein

\*Corresponding author. Department of Biochemistry, University of Oxford, South Parks Road, Oxford OX1 3QU, UK. Tel.: +44 1865 613 237; Fax: +44 1865 613 238; E-mail: david.sherratt@bioch.ox.ac.uk

<sup>3</sup>Present address: BG09, Biological Sciences, Faculty of Science and Information Technology, University of Newcastle, Callaghan, NSW, Australia.

Received: 18 December 2009; accepted: 12 February 2010

RecA (Chen *et al*, 2008). Intriguingly, some AAA+ motors have their six AAA+ domains naturally covalently linked into a single peptide (Vallee and Hook, 2006). This strategy allows us to introduce mutations into defined subunits and study the translocation properties of the mutated protein to understand how nucleotide binding and hydrolysis are coupled to translocation and the ability to do mechanical work. We demonstrate that covalent trimers dimerize to form hexamers that recognize KOPS, activate chromosome unlinking and translocate at velocities comparable to FtsK<sub>50C</sub>, the previously used translocase. Furthermore, we show that trimers with a catalytically inactive subunit at the central position form hexamers that have a normal translocation velocity but which are impaired in their ability to displace 'roadblocks' on DNA.

## Results

### FtsK translocase multimers are active *in vivo*

Most previous research on FtsK translocation *in vitro* has used a protein, FtsK<sub>50C</sub>, in which a 50 aa segment derived from the FtsK N-terminus has been added to the  $\alpha\beta\gamma$  translocase domain (Aussel *et al*, 2002; Ip *et al*, 2003; Saleh *et al*, 2004; Pease *et al*, 2005; Bigot *et al*, 2006). These 50 aa facilitate hexamerization and are required for significant *in vitro* catalytic activity (Aussel *et al*, 2002). Nevertheless, FtsK<sub>50C</sub> has a high propensity to aggregate, making quantitative biochemistry and mechanistic interpretation difficult. We reasoned that a minimal FtsK translocase, lacking the N-terminal 50 aa of FtsK<sub>50C</sub> and derived by using the available structure (Massey *et al*, 2006), might demonstrate *in vitro* activity if the individual monomers were covalently linked. Therefore, FtsK aa 840–1329 were linked together with a 14 aa linker (GGGSEGGGSEGGSG), thus forming covalent multimers of the translocase, the first subunit being tagged with a 6-His tag and/or biotin-tagged peptide (Figure 1).

In initial experiments, we showed that the gene, encoding a 320 kDa FtsK covalent hexamer, expressed well enough to give high levels of *in vivo* translocation-dependent XerCD-*dif* recombination (data not shown). Nevertheless, the level of expression was not sufficient to enable ready purification of the protein. Therefore, we chose to work with monomers, covalent dimers and covalent trimers (hereafter described as 'trimers'), which were expressed well. This provided the opportunity to introduce specific mutations into defined individual subunits of a covalent multimer. We then tested the *in vivo* activity of these translocases.

First, we exploited the observation that the overexpression of active FtsK translocase (e.g. FtsK<sub>50C</sub> when expressed from a *p<sub>ara</sub>* promoter with 0.2% arabinose) is toxic and cells stop growing and die within ~15 min of induced expression. Toxicity is correlated with the ability to hydrolyse ATP (Massey *et al*, 2006). Expression of monomer, dimer and trimer of the new FtsK translocase derivatives was toxic, consistent with them having *in vivo* activity (Table I). Cells stopped growing ~45 min after induced expression of the monomer, ~30 min after dimer expression and ~15 min after trimer expression, consistent with multimerization by covalent linking enhancing specific activity, because hexamers are the active species. Second, we tested whether the proteins could support *in vivo* XerCD-*dif* recombination on a reporter plasmid containing two *dif* sites (Recchia *et al*,

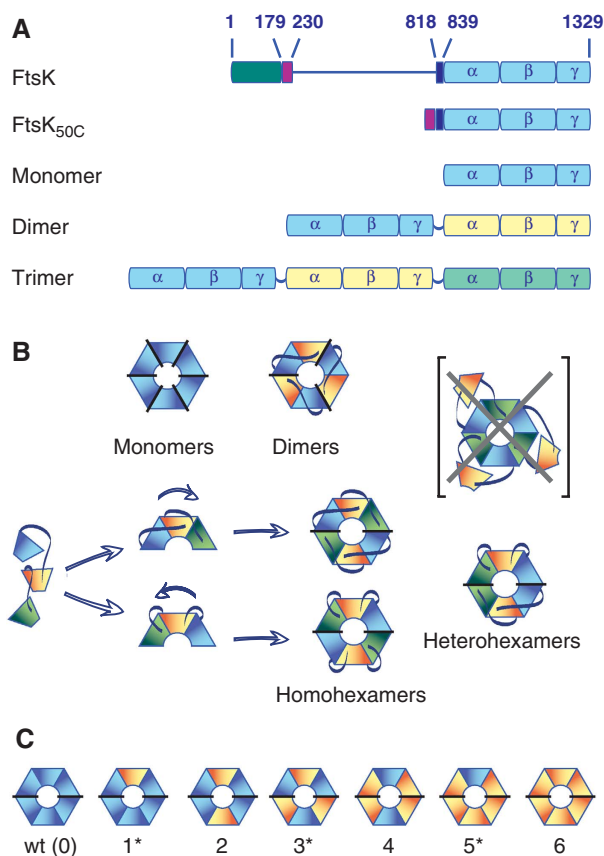


**Figure 1** (A) Schematic of the FtsK proteins used. FtsK depicts the wild-type protein, with four transmembrane helices in the N-terminus region (dark green), a 639 amino-acid linker (blue line) and the C-terminus motor domain (light blue boxes) is drawn, containing the three subdomains  $\alpha$ ,  $\beta$  and  $\gamma$ . FtsK<sub>50C</sub> is the soluble *E. coli* FtsK derivative that has been used in previous *in vitro* studies. The pink box represents the 50 aa segment derived from the linker, which is directly linked to the C-terminal motor. The dark blue box is a segment absent in the FtsK<sub>50C</sub> structure and in the derivatives used here: monomer, covalent dimers and covalent trimers. Subunits in covalent multimer derivatives are connected by a 14 aa linker, joining directly the C-terminus of the  $\gamma$ -subdomain to the first amino acid of the motor, L840. (B) Different potential configurations for multimer formation. The 14 aa linker is sufficiently short that we expect subunit 1 (blue) to be always adjacent to 2 (yellow), and subunit 3 (green) adjacent to 2 in the trimers. Nevertheless, it is plausible that two types of trimers can form, with the subunits folding in either a clockwise, or anticlockwise sequence. These can then potentially form mixed hexamers (heterohexamers) or unmixed hexamers (homohexamers). Because of the uncertainty of the configuration in trimers, mutations were introduced into either subunit 2 (single mutants), or subunits 1 and 3 (double mutants). In parentheses, with a cross, is shown how three covalent trimers with a centrally placed mutated subunit could conceivably form a hexamer with wild-type subunits and three looped out mutated subunits. We have no evidence that this can form. (C) Mutant hexamers. This figure depicts the mutants used in this study. Pure hexamers are obtained with a wild-type, single-mutant trimer, double-mutant trimer or triple-mutant trimer (0, 2, 4 or 6). Mixes of trimers are required to form hexamers with 1, 3 or 5 mutant subunits (marked with an asterisk). Mutated subunits are yellow and wild-type subunits are blue.

1999). The results of this assay mirrored the toxicity results; trimers were more active than covalent dimers, which were more active than monomers (Table I). These semi-quantitative assays do not take into account any differential levels of

**Table 1** *In vivo* activities of FtsK multimers

Assay	Monomer	Dimer	wt Trimer	2 WA <sup>a</sup>	4 WA	6 WA	2 WB	4 WB	6 WB
Toxicity <sup>b</sup> (min)	45	30	15	25	30	—	25	35	—
Recombination <sup>c</sup> (%)	25	50	60	63	12	17	58	24	24

<sup>a</sup>Hexamers formed by dimerization of trimers are described by the number of mutated WA or WB subunits.

<sup>b</sup>Toxicity was assayed as the time at which cell growth in LB ceases after FtsK induction with 0.2% arabinose. '—' indicates no toxicity.

<sup>c</sup>Recombination was measured *in vivo* on a reporter plasmid, 2 h after induction of FtsK expression by 0.02% arabinose. The values shown have the 0 min background subtracted.

these proteins in cells. Nevertheless, our extensive experience with these assays using FtsK<sub>50C</sub> derivatives (Sivanathan *et al*, 2006 and data not shown) has shown them to give a good indication of *in vitro* specific activity. We conclude that covalent trimers and dimers are highly active *in vivo*.

### ***In vitro* activities of FtsK translocase multimers**

The recombinant FtsK monomer, covalent dimer and trimer were then purified and assayed *in vitro* for ATPase activity and for two independent assays of DNA translocation: *in vitro* FtsK-dependent XerCD-*dif* recombination and triplex displacement assays (Figure 2; Aussel *et al*, 2002; Sivanathan *et al*, 2006). ATPase activity was DNA dependent (not shown), and at a concentration of 50 nM hexamer, the trimer hydrolysed  $>1.7 \times 10^3$  ATP/min/hexamer. At this protein concentration, the covalent dimers displayed ~80% of trimer specific activity, and the monomers ~1%, because of less efficient formation of active hexamers. The relatively low steady state level of ATP hydrolysis by the trimers indicates that most molecules are not translocating at any given time, presumably because they are not loaded onto DNA, have collided with other translocases, or are simply not active.

In XerCD-*dif* recombination and triplex displacement assays, the trimers were again the most active species, with covalent dimers showing ~40% of the activity of trimers. In the triplex displacement assays, optimal activity was obtained with trimers at 50 nM (hexamer), but required 80 and 150 nM for covalent dimers and monomers, respectively. These results confirm that covalent dimers and trimers are more active *in vitro* than the constituent monomers, with dimers and monomers forming hexamers at high and very high concentrations, respectively. In conclusion, trimers dimerize to form active hexamers efficiently at 50 nM, and their activity is higher than that observed for FtsK<sub>50C</sub> at the same concentration (Figure 1C and data not shown). Furthermore, the trimers were still responsive to the presence of KOPS in the triplex displacement and recombination assays (data not shown).

### **FtsK translocase trimers form hexamers on DNA**

Despite the trimers being highly active in translocation, we needed to be confident that the activity was resulting from dimerization of two trimers into a hexamer, rather than the activity residing in higher-order structures (Figure 1B, right panel), which could compromise interpretation of data once defined mutations had been introduced into the linked multimers. FtsK subunits were rendered non-functional by mutation in the highly conserved ATP-binding pocket. We used two mutations that have been shown to be catalytically defective in an extensive range of studies of RecA-fold proteins (ClpB: Watanabe *et al*, 2002; Dynein: Reck-Peterson and Vale, 2004; Rad51: Wiese *et al*, 2006 and archeal MCM:

Moreau *et al*, 2007). A K997A substitution in the Walker A box (WA) should prevent ATP binding, whereas a D1121A substitution in the Walker B box (WB) may allow ATP binding, but should be defective in ATP hydrolysis. Binding of trimers, containing 0 to 3 WA mutated subunits, to short KOPS-containing DNA was analysed by gel electrophoresis. Two shifted bands were observed in the presence of 200 nM protein, consistent with binding of one and two trimers on DNA (data not shown). Protein-DNA complexes containing wild-type, or three mutated WA subunits, were also observed by electron microscopy using negative staining. On a 2.7 kb DNA, particles whose shape and size were consistent with 'side-view' FtsK hexamers were the majority species (Figure 2E; Massey *et al*, 2006). The trapezium shape particles had diameters of 120–130 Å (large side) and 60–70 Å (small side). Aggregates or higher-order structures comprised <2% of particles. On a short DNA (44 bp), when 'end-on' view (top view) particles are expected, rounded particles of diameter ~130 Å were observed (Figure 2E), the size expected for a hexamer obtained by dimerization of trimers. However, we did not observe any lack of density corresponding to the central hole, or any six-fold symmetry (Massey *et al*, 2006). This may be because the  $\gamma$ -subdomains are attached to the  $\alpha\beta$  motor by a flexible linker, and therefore may occlude the central hole, as well as mask the symmetry of the protein complexes.

We then analysed whether the trimers could adopt alternative configurations when they dimerize into hexamers. The 14 aa linker may be long enough that it does not restrict the assembly into only a single configuration, although we expect the linker length to restrict the arrangement of subunits such that subunit 1 is never adjacent to subunit 3 (Figure 1B). The existence of alternative subunit configurations potentially complicates the interpretation of experiments using mutant subunits. To address this issue, we labelled His-tagged covalent trimers, pre-loaded onto short DNA to give preferential end-views, with 2 nm Ni-NTA-bound gold beads and assessed the relative locations of the beads within the hexamers by electron microscopy, followed by image classification (Figure 2G). The 1702 particles analysed were classified into 10, 50 or 100 groups on the basis of protein shape and gold position. Classes with two adjacent golds and with the two golds *in trans* were observed for each group, indicating that trimers can dimerize in both head-tail and head-head configurations (Figures 1B and 2G). However, some classes were ambiguous, with a very low signal-noise ratio, thereby precluding quantitative estimates of the two configurations. Given the likelihood that both configurations can form, we chose symmetrical configurations of mutations to avoid any ambiguity in the configurations of the subunits in the assembled hexamers. We focused most of our experiments on trimers containing a mutated subunit in the central

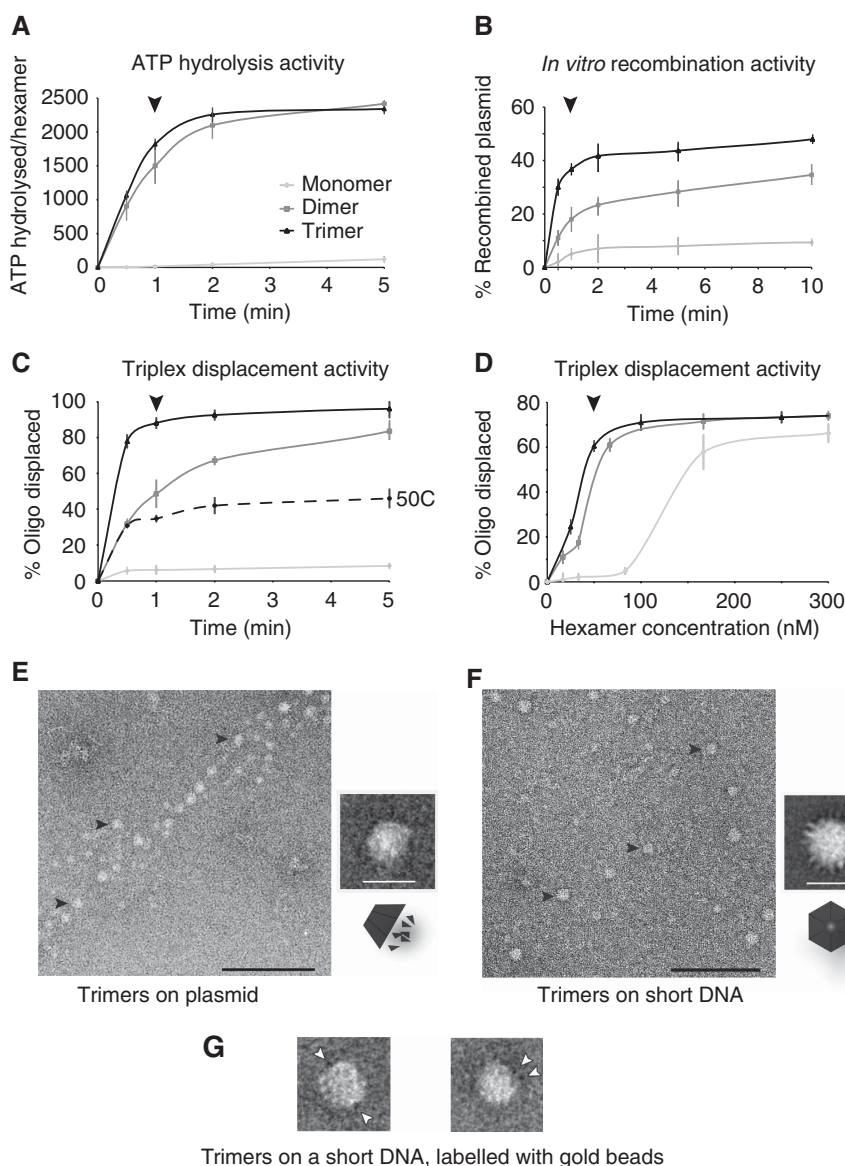


**Figure 2** *In vitro* activity of FtsK multimers. **(A)** ATP hydrolysis over time is shown for monomer, covalent dimer and trimer, at a concentration of 50 nM hexamer equivalent. The black arrow indicates the 1 min time point, which was used in later experiments (Figure 3). The mean data from three independent experiments, with standard deviations, are shown in panels **(A–D)**. **(B)** FtsK-dependent XerCD-*dif* recombination. Recombination was followed over time on a dimeric plasmid containing two *dif* sites lacking consensus KOPS-loading sites. Proteins (50 nM hexamer equivalent) were incubated with ATP and pre-bound XerCD, and the 1 min time point data (arrow) were used to generate the data in Figure 3. **(C)** Triplex displacement as a function of time; protein concentration was 50 nM (hexamer equivalent); the dotted line shows FtsK<sub>50C</sub> activity as a comparison. **(D)** Triplex displacement as a function of protein concentration; 1 min reactions were used to compare translocation activity of monomer, dimers and trimers over a range of 0–350 nM (hexamer equivalent). The activity does not increase with higher concentrations of protein (data not shown). **(E–G)** Electron microscopy of covalent trimers of FtsK on DNA. **(E)** A 2.7 kb, linearized plasmid, was used to study DNA binding by the trimers. A representative field using wild-type trimer is shown, as well as an averaged image of the protein seen from the side (162 particles), showing that the particles have the overall size expected for a hexamer composed of two trimers. Similar results were obtained with double and triple WA mutant trimers (data not shown). The black bar represents 100 nm, and the white bar 13 nm. Arrows point at examples of particles and a schematic of the side-on view is drawn under the averaged reconstructed image (inset). **(F)** Wild-type trimers were incubated with a 44 bp DNA-containing KOPS, thereby leading to preferential top-bottom views, giving an averaged reconstruction of particles of ~13 nm diameter (2600 particles selected) (inset). Similar results were obtained with double and triple WA mutant trimers (data not shown). Scale bars are the same as **(E)**. The schematic indicates the orientation of the particle on the grid. **(G)** Examples of gold labelling. Two classes averaged from a 100 group classification are shown, with beads on opposite sides of the particle (left) or side-by-side (right).

position, so that hexamers should carry two mutated subunits each separated by two wild-type subunits. Taken together, these results give us confidence that most biological activities assayed were the result of dimerization of trimers on DNA.

#### Activities of translocases with mutated subunits

To study coordination between FtsK subunits during DNA translocation, we compared the activities of presumptive hexamers derived from trimers with unmutated and/or mutated subunits. The mutations were introduced separately



into a given subunit of the trimers; in the central position to get a single mutant; in the first and the last subunits to get a double mutant and in all three subunits to get a triple mutant.

The mutated trimers were first tested *in vivo* using the toxicity and XerCD-*dif* recombination assays (Table I). In the toxicity assay, cells expressing the wild-type trimer showed a loss of exponential growth 15 min after induction of expression. Trimers containing three WA or three WB mutated subunits showed no toxicity and continued to grow. Trimers containing single WA or WB mutations were more toxic than trimers carrying two WA or WB mutations, with the trimer with two mutated WA subunits appearing slightly less toxic than its WB counterpart. The *in vivo* FtsK XerCD-*dif* recombination assays broadly mirrored the toxicity results, although in these assays, trimers with a single WA or WB mutant showed similar activity to wild-type trimers, whereas trimers with two WA or WB mutations appeared as deficient as trimers with three mutations. The residual level of recombination from the trimers with three mutated subunits may result from translocation-independent stimulation of recombination by the  $\gamma$ -subunits present on the trimers (Grainge I and Sherratt DJ, unpublished data).

Wild-type trimers were more active than wild-type covalent dimers in both of these assays, whereas wild-type monomers showed little if any activity. This result reassured us that any monomers or covalent dimers with one wild-type subunit and one mutated subunit, derived from proteolysis of trimers *in vitro* or *in vivo*, are unlikely to have significant activity that could confound the interpretation of the above experiments. These results gave us the confidence to purify the mutated trimers, giving the single, double and triple mutants in the WA and WB motifs, respectively (Figure 1).

### The FtsK translocation mechanism is neither stochastic nor strictly concerted

FtsK-dependent XerCD-*dif* site-specific recombination and displacement of a triplex-forming oligonucleotide were used to assay DNA translocation by the trimer variants and their combinations (Figure 3). For trimer mutants with 0, 1, 2 or 3 mutated subunits, we followed the decrease of recombination as a function of the number of mutant subunits. Assuming that the only potentially active species are hexamers formed by trimer dimerization, this gives data for hexamers with 0, 2, 4, or 6 mutated subunits. To obtain results for hexamers containing 1, 3 or 5 mutant subunits, different trimer mutants were mixed in equimolar amounts (Figure 1). For example, to obtain a hexamer population with only one mutated subunit, equal amounts of wild-type trimer and single-mutant trimer were mixed. In this mixture, it is predicted that 25% of hexamers are wild type; 50% carry a single mutated subunit; and 25% carry two mutated subunits. As the activity of each homo-hexamer is known, we were able to deduce the activity of the hetero-hexamer.

For the *in vitro* recombination assays that are dependent on DNA translocation by FtsK for activation of recombination, hexamers in which all of the subunits carry WA or WB mutations showed no activity, as expected, and gave us confidence that the mutations abrogate DNA translocation. By comparison, the wild-type subunits showed ~30% recombinant product in a 1 min reaction (Figure 2B; normalized to 100% in Figure 3).

Hexamers with two WA or WB mutations showed substantial recombination activity (~65% of wild type in 1 min reactions), whereas the mixed subunit population that gives hexamers with a single mutation (50%) showed at least wild-type activities after correction for the wild-type (25%) and double-mutated (25%) population. Some residual

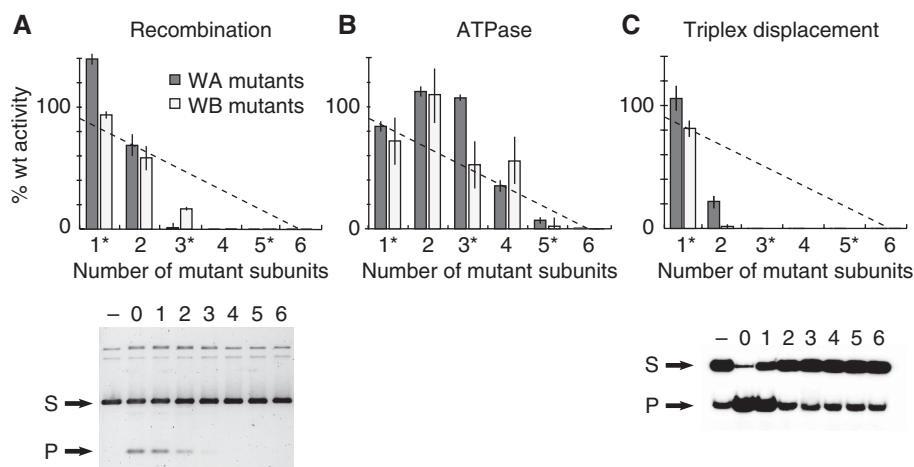


**Figure 3** *In vitro* activity of covalently linked mutated hexamers. (A) XerCD-*dif* recombination as a function of the number of mutated subunits. Recombination reactions were performed for 1 min on a dimeric plasmid containing two *dif* sites. In all, 50 nM hexamers were used on 27 nM 5.6 kb plasmid. % recombination is normalized to the activity of the wild-type (wt) hexamer, which gave ~30% recombination in 1 min (Figure 2). The dotted line shows the levels if there were a linear activity decrease as a function of increasing number of mutated subunits (A–C). The panel below shows an example of a recombination gel (0.8% agarose, 1 × TAE) for hexamers containing 0–6 WB mutated subunits (S) denotes recombination substrate; (P) denotes product; (–) denotes no FtsK. Error bars indicate standard deviation in three independent experiments, and asterisks indicate the combinations made by mixing appropriate trimers as in Figure 1C (A–C). (B) ATPase activity measured on a fraction of the recombination reaction shown in (A). Activity is normalized to that of the wild-type hexamer. (C) Triplex displacement. Triplex-displacement assays were carried out as in Figure 2. After subtracting background, activity was normalized to that of the wild-type hexamer. The panel below shows an example of a triplex reaction gel (4% acrylamide, 1 × TAM) for hexamers containing 0–6 WB mutants.

recombination activity (<20%) was observed in the assays in which 50% of the population should contain hexamers with three mutated subunits. No activity was observed with four mutated subunits. These observations are inconsistent with a stochastic firing model, in which a linear decrease in activity as a function of increasing mutated subunit number would be expected (Moreau *et al*, 2007). Similarly, obligate sequential rotary models, in which each subunit must be catalytically active in turn, can be ruled out, because a single-mutated subunit would block translocation. In parallel, ATPase activity was assayed in each of the recombination reactions, giving an estimate of the number of ATP consumed as a function of the level of recombination for each mutant hexamer (Figure 3B). Note that the absolute level of ATPase activity in the recombination assays cannot be compared directly with ATPase activity measured in the absence of recombinases, because the ATPase activity is downregulated when FtsK encounters XerCD bound to *dif* (Graham *et al*, 2010). ATPase activity decreased less sharply, with the four mutated subunit population retaining >40% of wild-type activity. This observation is consistent with an uncoupling of ATPase and translocation. Indeed by independent assays of ATPase activity under optimal conditions, with DNA in excess, there was an approximately linear decrease in ATPase activity as a function of the number of mutated subunits (data not shown). These results contrast to those from experiments in which wild-type *P. aeruginosa* FtsK (PAK4) hexamers were doped with increasing amounts of a WA mutant subunit and the ATPase activity measured (Massey *et al*, 2006). In that paper, there was a rapid, greater than linear reduction in ATPase activity as a function of mutated subunit concentration, leading to the conclusion of a rigorous sequential (or concerted) mechanism. However, we note that the absolute levels of ATPase activity were low, perhaps because a 16 bp dsDNA was used, which would not have supported significant DNA translocation. Furthermore, it is possible that the mutated subunits formed homohexamers and mixed hexamers more avidly than the wild-type protein on the 16 bp substrate, leading to an over-representation of hexamers containing  $\geq 3$  mutant subunits for a given input ratio.

In triplex-displacement assays, which provide an independent measure of translocation, hexamers with three or more mutant subunits all failed to show significant displacement activity in assays that required 60 bp of translocation after loading at KOPS, before encountering the triplex (Figure 3C). Hexamers with two WA or two WB mutated subunits showed  $\leq 20\%$  of wild-type activity, a marked contrast to their higher activity when activating Xer recombination. ATPase activities measured in the same reactions gave results similar to those in Figure 3B (data not shown). These data suggest a quantitative difference in 'readout' as compared with the recombination assays, perhaps because hexamers with mutated subunits are less able to displace a triplex when they have translocated up to it, as compared with being able to activate recombination after translocation up to the XerCD-*dif* complex. It is unlikely that the difference between assays reflects reduced processivity of translocation with mutated subunits, given that FtsK has to translocate only 60 bp in the triplex assay, whereas most random loadings of FtsK onto DNA in the recombination assay will leave >60 bp of translocation needed to encounter XerCD-*dif*. To test this directly, we

assayed translocation by wild-type and mutated trimers in a single-molecule assay.

### **Translocases with two catalytically inactive subunits show wild-type translocation velocity**

FtsK and its ortholog, SpoIIIE, have been shown to translocate along DNA at  $\sim 5$  kb/s and against forces of up to 60 pN, using single-molecule studies with both optical traps and magnetic tweezers (Saleh *et al*, 2004; Pease *et al*, 2005; Ptacin *et al*, 2008).

We used magnetic tweezers with a DNA molecule (17 kb, 5.7  $\mu$ m) tethered between the surface and a magnetic bead. The DNA was maintained in an extended conformation by magnets applying a constant force (Strick *et al*, 1996), to study translocation by hexamers derived from wild-type and mutated trimers. The FtsK variant and ATP were then added and the position of the bead was observed. Looping during translocation, probably arising when the translocase attaches to either the bead or the surface, causes the bead to move towards the surface during translocation. Either release of the loop or a reverse in translocation direction causes the bead to move away from the surface (Figure 4). These events can be distinguished by the rate of reversal of the bead. Between 360 and 930 events per protein were recorded, and the distributions of burst speeds were determined. Translocases derived from the wild-type trimer were first compared with FtsK<sub>50C</sub>. Both proteins showed the same translocation velocity (data not shown), with translocation events of several microns being common.

Translocases derived from trimers containing a mutated (WA or WB) central subunit were analysed in the same way and the average burst speed was deduced. Surprisingly, they translocated along DNA at rates similar to the wild-type covalent trimer against forces of 1–35 pN. The data shown were obtained at 5 pN and reveal a translocation velocity of  $\sim 3.3$  kb/s. We are confident that these events arise from the translocation of hexamers formed by dimerization of the mutated trimers, because our EM and gel-shift analysis provided no evidence for significant numbers of higher form multimers that could assemble six wild-type subunits into a hexamer (Figures 1 and 2). Also note that monomers and covalent dimers were not active at this concentration. Furthermore, the observation of substantial translocation activity by the covalent trimers with a single-mutated subunit in the XerCD-*dif* recombination reaction, where specific activity can be estimated, reinforces our conclusion that hexamers with mutated subunits in the 2 and 5 positions exhibit wild-type translocation rates. This led us to wonder whether the low activity in the triplex-displacement assays results from a failure to displace the triplex efficiently rather than an impaired ability to translocate up to the triplex. This could mean that the covalent trimer with a central mutant subunit would have an impaired ability to generate the mechanical work required to displace the triplex, despite a normal translocation velocity.

Magnetic tweezers are not a good tool to measure and compare FtsK stall forces as both processivity and events rate dramatically decrease at high force (Saleh *et al*, 2004; Pease *et al*, 2005), while modification of DNA structure at high forces may affect the results. This led us to use another strategy.

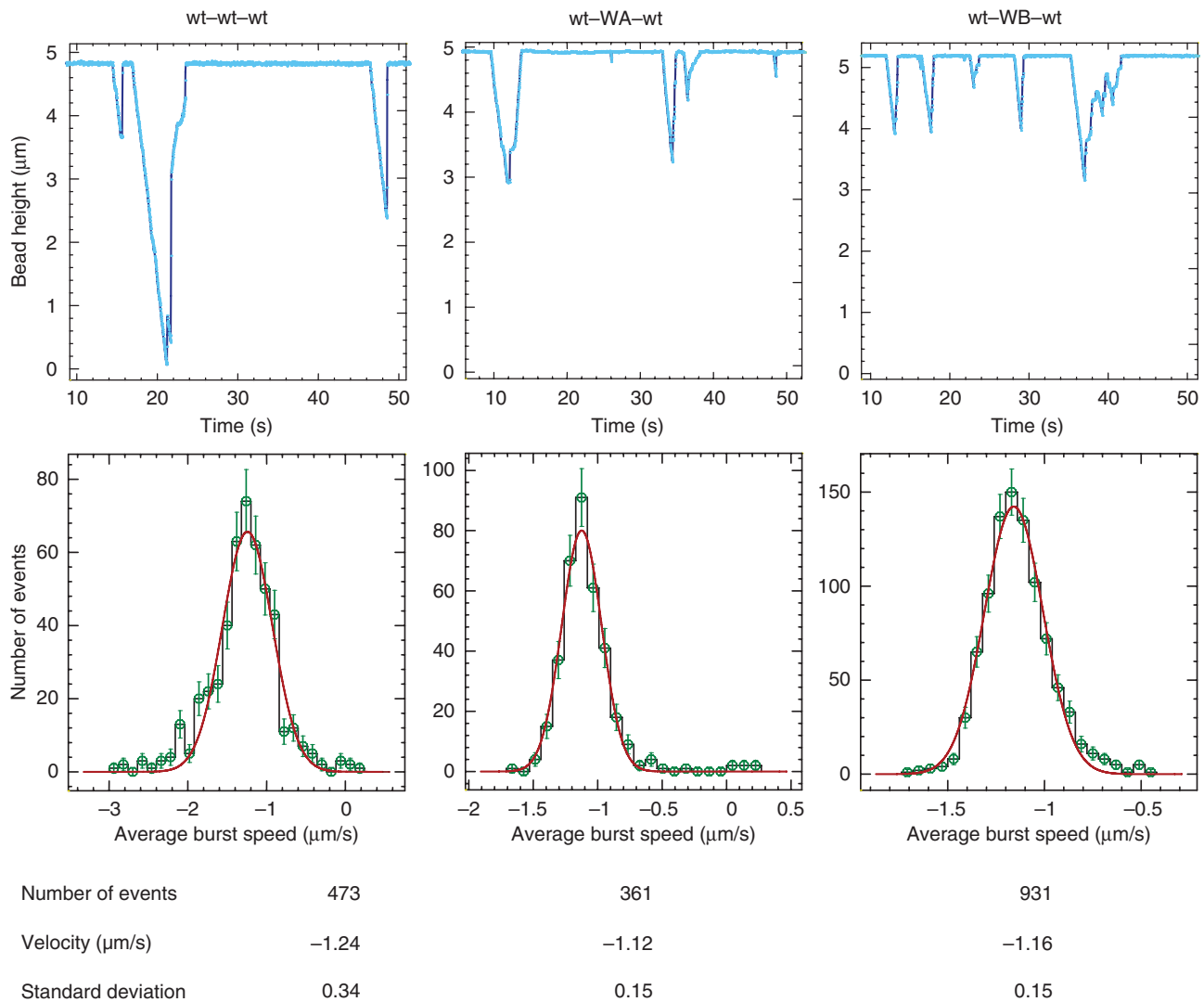


**Figure 4** Single-molecule analysis of covalent multimer translocation. Magnetic tweezers were used to study translocation of wild-type and double mutant hexamers, containing WA or WB in the central subunit of the trimers. Upper panels show examples of events obtained for each protein. There is no statistical significance to the relative lengths of the events shown. Light blue, data points; dark blue, fit to the data points. Lower panels show the distribution of average burst speed. The number of events, the average burst speed and its distribution are plotted under each panel. Green, data points, with s.d. (bars); red, Gaussian fits to the data. Note that the WA derivative shown here is biotin tagged and will, therefore, associate with the bead. A His-tagged derivative showed similar velocities. The data shown were obtained at a force of 5 pN and 2 mM ATP.

#### **Trimers with a single catalytic mutation give translocases impaired in displacing a DNA roadblock**

To calibrate the relative ability of molecular motors to strip streptavidins from DNA, we have generated a panel of mutated streptavidins with a wide range of off-rates from biotin (Chivers *et al*, 2010). The streptavidin-biotin interaction is one of the strongest non-covalent interactions characterized, with a  $K_D$  of  $\sim 4 \times 10^{-14}$  M (Green, 1990). Here, we focused on one stronger mutant and one weaker mutant of streptavidin. The stronger streptavidin mutant had a 10-fold lower off-rate from biotin ( $< 2\%$  spontaneous dissociation from biotin-4-fluorescein in 12 h) than wild-type streptavidin (12% spontaneous dissociation in 12 h). The weaker mutant had accelerated dissociation from biotin conjugates (Supplementary Figure S1), but binding was still strong enough to survive gel electrophoresis.

Therefore, to examine the ability of FtsK to do mechanical work to displace roadblocks on DNA during translocation, we

compared the ability of wild-type and mutated trimers to displace wild-type and mutated streptavidins from biotinylated DNA. A 597 bp DNA fragment biotinylated at one end and with two KOPS sites positioned 230 bp upstream was bound by streptavidin and used in FtsK translocation assays. After 2 min reactions with translocase and ATP, agarose gel electrophoresis was used to analyse the fraction of DNA molecules where streptavidin had been displaced. Excess free biotin was used as a 'sink' to prevent rebinding of displaced streptavidin and 0.1% SDS was used to stop translocation, conditions that do not denature streptavidin (Figure 5). Wild-type hexamers displaced  $> 70\%$  of streptavidin in 2 min, whereas translocases with two WA or WB mutations displaced  $< 45\%$  of streptavidin. In all, 30% of the tight-binding streptavidin was displaced in 2 min by the wild-type trimer, whereas  $\leq 10\%$  was displaced by the singly mutated trimers. In contrast, the weaker streptavidin was displaced to comparable levels ( $\geq 82\%$ ) by all three proteins,

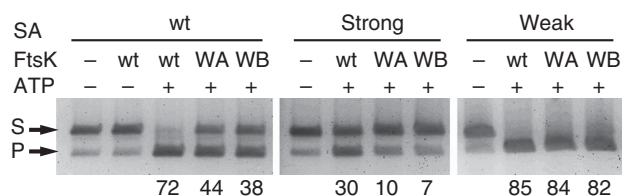


**Figure 5** Displacement of the streptavidin ‘roadblock’ during translocation. Streptavidin displacement activity was followed on a 597 bp biotinylated DNA. Excess streptavidin (wt, strong, or weak binding derivatives) was bound for 30 min and then excess free biotin was added. The indicated trimers (WA and WB contained mutations in the central subunit; 250 nM hexamer) were added, followed by ATP, and the reactions were stopped after 2 min. % displacement (determined by gel electrophoresis; 1.5% agarose/TBE; background subtracted) is indicated. Independent repetitions ( $\geq 2$ ) gave comparable results. (S) substrate; (P) product.

showing that they have comparable abilities to translocate up to, and displace, a weak roadblock. Taken together, these data show that trimers with one catalytically inactive subunit form translocases as rapid as those formed by wild-type trimers, but which are impaired in displacing strong roadblocks that include triplex DNA and streptavidin bound to biotin.

## Discussion

The construction of functional FtsK covalent multimers has provided robust new dsDNA translocases that still recognize KOPS-loading sites on DNA and activate XerCD recombination at *dif*. The use of covalent multimers has revealed new insight into the catalytic mechanism of FtsK and has demonstrated that translocation velocity can be uncoupled from the ability to actively remove roadblocks on DNA. Covalent trimers dimerize efficiently to form biologically active hexamers. We found little formation of higher-order multimers that would complicate the interpretation of the data. Covalent trimers containing catalytic mutations in the central position formed translocases with normal translocation velocities at forces at least up to 10 pN, and were able to translocate over 1 or 2  $\mu\text{m}$  in a single processive event. Nevertheless, these mutated translocases were compromised in their ability to displace streptavidin from biotinylated DNA or a triplex oligonucleotide. The ability to separate translocation velocity from force generation in displacing a potential ‘roadblock’ has mechanistic implications and substantiates our belief that we are not forming a wild-type hexamer within a higher-order structure that has catalytically inactive subunits positioned outside of the functional hexamer (Figure 1B). This is the first study that we are aware of that uses covalently linked multimers to study a hexameric DNA translocase, although mechanistic and structural studies of the hexameric ClpX protein-unfolding machine and of RecA have used covalently linked subunits (Martin *et al*, 2005; Chen *et al*, 2008; Glynn *et al*, 2009).

### The FtsK translocation mechanism

Historically, three types of mechanism have been considered for the translocation of ring-shaped translocases and helicases (Singleton *et al*, 2007; Thomsen and Berger, 2009). Stochastic mechanisms require that subunits in a ring ‘fire’ randomly, and such a mechanism has been proposed to operate during protein unfolding by ClpX (Martin *et al*,

2005). A concerted mechanism, in its most rigorous form, requires that all potentially active subunits fire simultaneously. Although a concerted mechanism has been proposed for the translocase action of SV40 T antigen (Gai *et al*, 2004), there is no compelling evidence to believe that such a mechanism operates widely. In contrast, sequential, ‘binding change’ models for translocation receive extensive support. In these, an asymmetry in the ring, as a consequence of different nucleotide-binding states, is propagated around the ring as DNA or RNA is translocated through the ring. The F1 ATPase provides the paradigm for such a rotary motor, although in this case only three of the six subunits in the ring are catalytically active (Zhou and Boyer, 1993); experimental data derived from studies of a number of helicases and translocases lend support to such a mechanism (reviewed in Singleton *et al*, 2007; Enemark and Joshua-Tor, 2008). Structures of the T7 gp4 helicase in the absence of DNA revealed asymmetric nucleotide-binding states within the ring and led to a ‘hand-off’ model in which each subunit changes its nucleotide contacts with each catalytic step (Singleton *et al*, 2000; Figure 6A). Subsequent studies of the same protein led to the conclusion that the catalytic mechanism required that all six subunits be catalytically active for translocation to occur, as doping of wild-type protein with a catalytic mutant had an immediate and dramatic effect on DNA-dependent nucleotide hydrolysis; nevertheless, unscheduled ATP hydrolysis in the absence of DNA continued with stochastic firing of catalytically competent subunits (Crampton *et al*, 2006).

Subsequently, a rotary hand-off translocation mechanism for FtsK was proposed on the basis of structural studies, with the suggestion that 2 bp are translocated per catalytic step, with a rotational resetting after each step to accommodate the difference between the normal 10.5 bp per helical turn of B DNA and the 12 bp proposed to be translocated in a complete hexamer catalytic cycle (Massey *et al*, 2006). This resetting can explain the modest level of (+) DNA supercoiling that accumulates ahead of the translocase (Saleh *et al*, 2005). If this mechanism operates during FtsK translocation, the observation that hexamers with two catalytic mutations show normal velocity suggests that the mechanism can accommodate a now substantial rotational (or translational) resetting to locate the next active subunit. Such a major resetting without influence on translocation velocity seems unlikely and is inconsistent with a strict hand-off sequential mechanism. It would also imply that nucleotide binding or release rather than the chemical steps would be rate limiting in such semi-sequential translocation.

More recently, structural studies of E1 papillomavirus helicase (Enemark and Joshua-Tor, 2006) and RNA translocase Rho (Thomsen and Berger, 2009) revealed more incisive mechanistic insight into the translocation process, because the structures showed the asymmetry and different nucleotide-binding states required for a sequential-binding site change mechanism. In each of these cases, a spiral staircase of loops protrudes into the central channel, with each loop grasping the phosphodiester backbone, in a way that can help propel the nucleic acid with respect to the protein. Both of these structures support an ‘escorted translocation’ mechanism, rather than a hand-off mechanism (Figure 6). In the Rho mechanism, six nucleotides of ssRNA occupy the channel, with each nucleotide potentially being bound by a loop



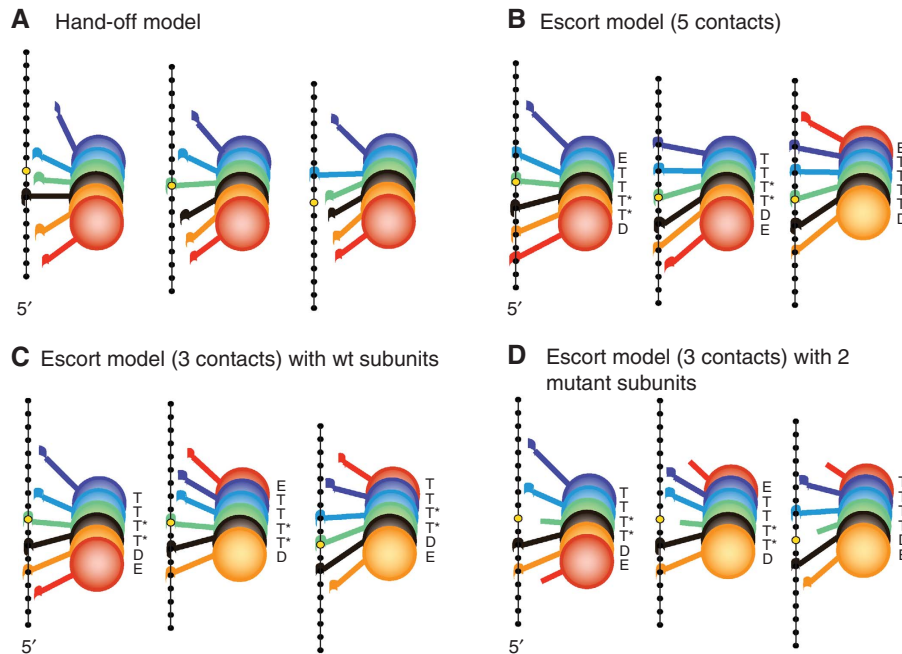


**Figure 6** Translocation models. Scheme of FtsK translocation on DNA. The six subunits are drawn as spheres with a paddle representing the loop(s) in the  $\alpha$  and/or  $\beta$  domains interacting with DNA nucleotides (black dots). One nucleotide is taken as a reference to show relative movement (yellow dot). Subunits inactivated by WA or WB catalytic mutations are indicated by a shorter paddle without the hook. Note that to simplify the drawing, subunits are represented linearly, but in reality would form a ring around DNA. **(A)** A sequential hand-off mechanism as applied to FtsK. In this model, all protein subunits change their local association with a given DNA segment, whether it be through specific contacts or not, during each chemical step (Massey *et al*, 2006; Enemark and Joshua-Tor, 2008). Each catalytic step leads to 2 bp dsDNA translocated. **(B)** Sequential escort model, as applied to FtsK. In this class of model, only one of the subunits changes its DNA contacts at each catalytic step and flexibility in the subunits and their loops allows movement of one subunit from the bottom to the top of the staircase during each catalytic step (Enemark and Joshua-Tor, 2008; Thomsen and Berger, 2009). In this panel, five of the six subunits are contacting every other nucleotide to avoid the substantial overwinding required to contact adjacent nucleotides. This model would require  $>30 \text{ \AA}$  movement of a subunit, as it moves from the bottom to the top of the staircase. The indicated nucleotide states of the subunits are; T, ATP bound; T\*, ATP transition state; D, ADP bound; E, 'exchange' (nucleotide free) (Thomsen and Berger, 2009). **(C)** Escort model with three subunit–nucleotide interactions, each occurring every other nucleotide. In this case, the movement of subunits and their loops during transition from the bottom to the top of the staircase would be similar to that for Rho/E1 ( $\sim 15 \text{ \AA}$ ). **(D)** Escort model in a hexamer containing two mutated subunits. At least two protein–DNA contacts are still feasible in this situation, allowing velocity to remain the same, but reducing the work available to displace roadblocks.

derived from each subunit of the hexamer. After ATP hydrolysis, phosphate is eventually released to give a subunit that loses its strong association with nucleic acid. On ADP release or ATP binding, a subunit loop switches position from the bottom to the top of the staircase, grabbing the 3' nt immediately ahead of the protein and only releasing the nucleotide six catalytic steps (i.e. one complete catalytic cycle) later; this requires a  $\sim 15 \text{ \AA}$  movement of the loop. In the Rho structure, which has the nucleotide mimic ADP-BeF<sub>3</sub> bound to each subunit, there are two 'ATP-bound' states (T), two 'ATP-bound' transition states (T\*), an 'ADP state' (D) and an exchange (E; nucleotide-free) state, organized in an anti-clockwise manner as one views from the 5' end of the RNA; intersubunit interactions are strongest in the transition state interface and weakest surrounding the exchanging subunit (Thomsen and Berger, 2009). Such a scheme can be applied to FtsK, although the substantial overwinding of duplex DNA in the FtsK hexameric channel, required if there were to be one set of nucleotide contacts per FtsK subunit, seems unlikely. An alternative would be to have one FtsK subunit per two nucleotides, with five contacts at any one time, giving 2 bp translocated per catalytic step and close to normal (or somewhat underwound) B DNA in the channel (Figure 6B). If this were the case, movements in the loop-contacting DNA

in the protein subunit that switches position in a given step would need to span  $>30 \text{ \AA}$  of DNA, twice as large as in Rho or E1. However, if only a subset of subunits (Figure 6C) make a DNA contact at any time, then the catalytic cycle could be accommodated with movements similar to those observed for Rho/E1.

An escort model for FtsK translocation can accommodate our observation of normal velocity yet reduced ability to displace roadblocks when two catalytically inactive subunits are introduced into a hexamer. This is because coordinated cooperative interactions within the hexamer and with DNA potentially allow a subunit interface to bypass the active configuration without hydrolysing ATP (Figure 6D). Normal velocity is possible because the chemical steps are not rate limiting and/or because a 'Brownian ratchet' allows the bypass without a diminution in velocity. Nevertheless, a hexamer with two ATP non-hydrolysing subunits would be expected to be able to do less work in displacing a roadblock than a hexamer in which all subunits are catalytically competent, consistent with our observations. It is noteworthy that several hexameric rotary motors have evolved to have a mixture of inactive and active subunits, notably F1 ATPase and dynein. We note that the phage  $\phi 12$  P4 hexameric pump, which belongs to the RecA-family, also

seems to use an escort mechanism for ssRNA translocation into the capsid, although in this case it appears that three consecutive nucleotide-bound subunits contact RNA and cooperate in catalysis (Mancini *et al*, 2004; Kainov *et al*, 2008).

Further understanding of the FtsK mechanism will require the combination of structural, biochemical, genetic and single-molecule studies. As yet, we have failed to obtain high-resolution structures of FtsK with DNA, which may reveal the predicted asymmetry in structure and nucleotide-binding state for a sequential-binding change model. Although single-molecule studies have been invaluable in analysing translocation speeds, processivities and directionality of translocation, the rapid speed of translocation has precluded obtaining data on individual catalytic step sizes. Similarly, our attempts to measure the amount of ATP consumed per bp of DNA translocated have had insufficient resolving power, given the speed of translocation (Graham JE and Sherratt DJ, unpublished data).

Finally, the types of study reported here need to be extrapolated to the *in vivo* temporal and spatial behaviour of FtsK in the final stages of chromosome segregation. *In vivo*, FtsK translocation must not be hindered by potential roadblocks on DNA, as FtsK needs to translocate from wherever it loads to XerCD-bound *dif* sites, where translocation stops and the final chromosome unlinking is activated. The ability of FtsK to efficiently displace streptavidin from biotin-DNA suggests that it is an efficient remover of roadblocks *in vivo*. The observation that FtsK hexamers with two mutated subunits can translocate with normal velocity yet are compromised in displacing roadblocks on DNA, also raises the possibility that *in vivo* FtsK translocation can occur in a mode that allows fast translocation without all subunits firing in each complete catalytic cycle, with the full catalytic potential only realized when roadblocks need to be removed during translocation.

## Materials and methods

### Strains and plasmids

*E. coli* DS9041 (FtsK<sub>C</sub>) was used to express alleles of *ftsK* in *in vivo* recombination experiments (Recchia *et al*, 1999). *E. coli* BL21 was used to overexpress FtsK derivatives. All *ftsK* alleles were cloned into plasmid pBAD24, under an arabinose-inducible promoter and with an N-terminal 6His-tag (Guzman *et al*, 1995). Plasmid pFX142 is a pSC101 derivative containing two *dif* sites (Aussel *et al*, 2002). Kanamycin (50 µg/ml), ampicillin (100 µg/ml) and spectinomycin (25 µg/ml) were used when required. The C-terminus motor of FtsK was cloned from nucleotide 2518 to 3987, or 3990 when the stop codon was required. The monomer was cloned into pBAD24 between *EcoRI* and *HindIII* sites. The dimer contained the first subunit cloned between *EcoRI* and *XbaI* restriction sites, and the second between *XbaI* and *HindIII* sites. The two repeats were joined together by the sequence coding for the 14 amino-acid linker (GGGSEGGGSEGGG): 5'-GCGGCGTTCCGAGGGCGGTGGTTCCAG AAGGCGGTTCCGGT-3', followed by the *XbaI* restriction site. Trimers were designed the same way with three fragments cloned between *EcoRI*, *XbaI*, *KpnI* and *HindIII* sites, the last one containing the stop codon before the *HindIII* site.

### Toxicity and *in vivo* recombination

Plasmids containing *ftsK* alleles were transformed into DS9041 and cells were grown in LB-glucose to avoid expression from *p<sub>ara</sub>*. Overnight cultures were diluted 1/100 in LB, and FtsK expression was induced at A<sub>600</sub> 0.5 by 0.2% arabinose (3 h; 37°C).

Recombination was assayed as in Sivanathan *et al* (2006).

### Protein purification

FtsK derivatives were purified as in Massey *et al* (2006), with purification through Talon resin, heparin and Q-HP columns (GE Healthcare). XerC and XerD were purified as in Subramanya *et al* (1997). Streptavidin variants were purified as in Howarth and Ting, 2008.

### ATPase, *in vitro* recombination and triplex-displacement assays

These were as described in Massey *et al* (2006) and Sivanathan *et al* (2006), respectively. Reaction buffer (RB) was 25 mM Tris pH 7.5, 10 mM MgCl<sub>2</sub>; ATPase assays were carried out on a supercoiled, 9 kb plasmid and *in vitro* recombination on a dimeric plasmid derived from pMin33, which contains a *dif* site.

### Electron microscopy and image processing

Protein samples and DNA were mixed at a ratio of 1 hexamer per 66 bp, or 1 per 54 bp for the short DNA and plasmid, respectively, in binding buffer (BB: 25 mM Tris pH 7.5, 30 mM NaCl and 5 mM MgCl<sub>2</sub>). The protein-DNA samples were then applied to electron microscope hydrophilic grids coated with carbon film and stained with 2% uranyl acetate. The preparations were examined using a Philips CM120 electron microscope equipped with a LaB<sub>6</sub> filament, with an acceleration voltage of 120 kV. Electron micrographs were taken at a magnification of ×45 000 at low dose. Selected images were digitized with a step size of 12.5 mm on a Super Coolsan 9000 Nikon. The WEB and SPIDER software package (Frank *et al*, 1996) was used for all image processing. In all, 162 particles on plasmid and 2600 on short DNA were windowed, centred and aligned using the reference-free alignment procedure. For the gold labelling, 3 µl FtsK-DNA complex were applied on glow discharged carbon-coated grids. The grid was washed after 1 min with BB and incubated with Ni-NTA Nanogold (Nanoprobes) solution (5 µM Ni-NTA Nanogold in BB) for 4 min at 25°C. The grid was rinsed twice on drops of BB and stained with 2% uranyl acetate. In all, 1702 particles were windowed and subjected to reference-free alignment and sorted into 10, 50 or 100 classes using K-means clustering (Frank, 1990). A control was made using the same protocol as above but BB was used instead during the labelling step, and no significant difference was observed as for the shape and size of the particles.

### Magnetic tweezer assays

Single-molecule experiments were performed with magnetic tweezers (Strick *et al*, 1996). Permanent magnets provided a constant force that varied from 1 to 10 pN in most experiments, although a few experiments were carried out at 35 pN. DNA (pFX355, 17 kb, gift from FX Barre) and surfaces were prepared as described in Lionnet *et al* (2008). Experiments were performed in a buffer containing 2 mM ATP, 10 mM Tris pH 7.6, 150 mM NaCl and 10 mM MgCl<sub>2</sub>. FtsK was added until translocation events were observed (typically 50 nM). For each translocation event, speed was obtained from a linear fit to the DNA extension versus time data. For each DNA molecule on a given condition, the individual translocation events were pooled and a histogram of the translocation speed was built, then fitted to a Gaussian function.

### Streptavidin-displacement assays

DNA fragments (597 bp) were generated by PCR, using a 5' biotinylated oligonucleotide primer on a plasmid template containing two non-overlapping KOPS pointing towards the biotinylated end. This was first incubated with 0.5 µM streptavidin analogues in RB for 20 min, then 0.1 mM biotin was added as a sink before FtsK (250 nM hexamer). After 2 min incubation, 2 mM ATP was added. Reactions were run at 25°C for 2 min, stopped with 0.1% SDS, 20 mM EDTA pH 8 and loaded on a 1.5% agarose gel in TBE 1 ×. Gels were run at 4°C, 100 V for 90 min and visualized and quantitated as above.

### Supplementary data

Supplementary data are available at *The EMBO Journal* Online (<http://www.embojournal.org>).

## Acknowledgements

The work in Oxford was supported by the Wellcome Trust (EC, IG, CV-B, MH and DJS) and the BBSRC (CEC). In Paris, the work was


supported by the Wellcome Trust (EC), ANR, IUF and an EU grant, Bionanoswitch (AM and J-FA). We thank many of our mechanistic biochemistry colleagues for invaluable discussions.

## References

- Aussel L, Barre FX, Aroyo M, Stasiak A, Stasiak AZ, Sherratt D (2002) FtsK is a DNA motor protein that activates chromosome dimer resolution by switching the catalytic state of the XerC and XerD recombinases. *Cell* **108**: 195–205
- Begg KJ, Dewar SJ, Donachie WD (1995) A new *Escherichia coli* cell division gene, *ftsK*. *J Bacteriol* **177**: 6211–6222
- Bigot S, Saleh O, Cornet F, Allemand J, Barre F (2006) Oriented loading of FtsK on KOPS. *Nat Struct Mol Biol* **13**: 1026–1028
- Chen Z, Yang H, Pavletich NP (2008) Mechanism of homologous recombination from the RecA-ssDNA/dsDNA structures. *Nature* **453**: 489–494
- Chivers CE, Crozat E, Chu C, Moy VT, Sherratt DJ, Howarth M (2010) A streptavidin variant with slower biotin dissociation and increased mechanostability. *Nat Methods* (in press; doi:10.1038/nmeth.1450)
- Crampton D, Mukherjee S, Richardson C (2006) DNA-induced switch from independent to sequential dTTP hydrolysis in the bacteriophage T7 DNA helicase. *Mol Cell* **21**: 165–174
- Dorazi R, Dewar SJ (2000) Membrane topology of the N-terminus of the *Escherichia coli* FtsK division protein. *FEBS Lett* **478**: 13–18
- Enemark EJ, Joshua-Tor L (2006) Mechanism of DNA translocation in a replicative hexameric helicase. *Nature* **442**: 270–275
- Enemark EJ, Joshua-Tor L (2008) On helicases and other motor proteins. *Curr Opin Struct Biol* **18**: 243–257
- Frank J (1990) Classification of macromolecular assemblies studied as ‘single particles’. *Q Rev Biophys* **23**: 281–329
- Frank J, Radermacher M, Penczek P, Zhu J, Li Y, Ladjadj M, Leith A (1996) SPIDER and WEB: processing and visualization of images in 3D electron microscopy and related fields. *J Struct Biol* **116**: 190–199
- Gai D, Zhao R, Li D, Finkielstein CV, Chen XS (2004) Mechanisms of conformational change for a replicative hexameric helicase of SV40 large tumor antigen. *Cell* **119**: 47–60
- Glynn SE, Martin A, Nager AR, Baker TA, Sauer RT (2009) Structures of asymmetric ClpX hexamers reveal nucleotide-dependent motions in a AAA+ protein-unfolding machine. *Cell* **139**: 744–756
- Graham JE, Sivanathan V, Sherratt DJ, Arciszewska LK (2010) FtsK translocation on DNA stops at XerCD-*dif*. *Nucleic Acids Res* **38**: 72–81
- Grainge I, Bregu M, Vazquez M, Sivanathan V, Ip SC, Sherratt DJ (2007) Unlinking chromosome catenanes *in vivo* by site-specific recombination. *EMBO J* **26**: 4228–4238
- Green NM (1990) Avidin and streptavidin. *Methods Enzymol* **184**: 51–67
- Guzman LM, Belin D, Carson MJ, Beckwith J (1995) Tight regulation, modulation, and high-level expression by vectors containing the arabinose  $p_{BAD}$  promoter. *J Bact* **177**: 4121–4130
- Howarth M, Ting AY (2008) Imaging proteins in live mammalian cells with biotin ligase and monovalent streptavidin. *Nat Protoc* **3**: 534–545
- Ip SC, Bregu M, Barre FX, Sherratt DJ (2003) Decatenation of DNA circles by FtsK-dependent Xer site-specific recombination. *EMBO J* **22**: 6399–6407
- Kainov DE, Mancini EJ, Telenius J, Lissal J, Grimes JM, Bamford DH, Stuart DI, Tuma R (2008) Structural basis of mechanochemical coupling in a hexameric molecular motor. *J Biol Chem* **283**: 3607–3617
- Lionnet T, Allemand JF, Revyakin A, Strick TR, Saleh OA, Bensimon D, Croquette V (2008) Single-molecule studies using magnetic traps. In *Single-Molecule Techniques: a Laboratory Manual*, Selvin PR, Ha T (eds). Cold Spring Harbor, NY: Cold Spring Harbor Laboratory Press
- Mancini EJ, Kainov DE, Grimes JM, Tuma R, Bamford DH, Stuart DI (2004) Atomic snapshots of an RNA packaging motor reveal conformational changes linking ATP hydrolysis to RNA translocation. *Cell* **118**: 743–755
- Martin A, Baker T, Sauer R (2005) Rebuilt AAA+ motors reveal operating principles for ATP-fuelled machines. *Nature* **437**: 1115–1120
- Massey T, Mercogliano C, Yates J, Sherratt D, Lowe J (2006) Double-stranded DNA translocation: structure and mechanism of hexameric FtsK. *Mol Cell* **23**: 457–469
- Moreau M, McGeoch A, Lowe A, Itzhaki L, Bell S (2007) ATPase site architecture and helicase mechanism of an archaeal MCM. *Mol Cell* **28**: 304–314
- Pease PJ, Levy O, Cost GJ, Gore J, Ptacin JL, Sherratt D, Bustamante C, Cozzarelli NR (2005) Sequence-directed DNA translocation by purified FtsK. *Science* **307**: 586–590
- Ptacin J, Nollmann M, Becker E, Cozzarelli NR, Pogliano K, Bustamante C (2008) Sequence-directed DNA export guides chromosome translocation during sporulation in *Bacillus subtilis*. *Nat Struct Mol Biol* **15**: 485–493
- Recchia GD, Aroyo M, Wolf D, Blakely G, Sherratt DJ (1999) FtsK-dependent and -independent pathways of Xer site-specific recombination. *EMBO J* **18**: 5724–5734
- Reck-Peterson SL, Vale RD (2004) Molecular dissection of the roles of nucleotide binding and hydrolysis in dynein’s AAA domains in *Saccharomyces cerevisiae*. *Proc Natl Acad Sci USA* **101**: 1491–1495
- Saleh O, Bigot S, Barre F, Allemand J (2005) Analysis of DNA supercoil induction by FtsK indicates translocation without groove-tracking. *Nat Struct Mol Biol* **12**: 436–440
- Saleh O, Pérals C, Barre F, Allemand J (2004) Fast, DNA-sequence independent translocation by FtsK in a single-molecule experiment. *EMBO J* **23**: 2430–2439
- Singleton MR, Dillingham MS, Wigley DB (2007) Structure and mechanism of helicases and nucleic acid translocases. *Annu Rev Biochem* **76**: 23–50
- Singleton MR, Sawaya MR, Ellenberger T, Wigley DB (2000) Crystal structure of T7 gene 4 ring helicase indicates a mechanism for sequential hydrolysis of nucleotides. *Cell* **101**: 589–600
- Sivanathan V, Allen M, De Bekker C, Baker R, Arciszewska L, Freund S, Bycroft M, Löwe J, Sherratt D (2006) The FtsK  $\gamma$  domain directs oriented DNA translocation by interacting with KOPS. *Nat Struct Mol Biol* **13**: 965–972
- Steiner W, Liu G, Donachie WD, Kuempel P (1999) The cytoplasmic domain of FtsK protein is required for resolution of chromosome dimers. *Mol Microbiol* **31**: 579–583
- Strick TR, Allemand JF, Bensimon D, Bensimon A, Croquette V (1996) The elasticity of a single supercoiled DNA molecule. *Science* **271**: 1835–1837
- Subramanya HS, Arciszewska LK, Baker RA, Bird LE, Sherratt DJ, Wigley DB (1997) Crystal structure of the site-specific recombinase, XerD. *EMBO J* **16**: 5178–5187
- Thomsen ND, Berger JM (2009) Running in reverse: the structural basis for translocation polarity in hexameric helicases. *Cell* **139**: 523–534
- Vallee RB, Hook P (2006) Autoinhibitory and other autoregulatory elements within the dynein motor domain. *J Struct Biol* **156**: 175–181
- Watanabe YH, Motohashi K, Yoshida M (2002) Roles of the two ATP binding sites of ClpB from *Thermus thermophilus*. *J Biol Chem* **277**: 5804–5809
- Wiese C, Hinz JM, Tebbs RS, Nham PB, Urbin SS, Collins DW, Thompson LH, Schild D (2006) Disparate requirements for the Walker A and B ATPase motifs of human RAD51D in homologous recombination. *Nucleic Acids Res* **34**: 2833–2843
- Yu XC, Weihe EK, Margolin W (1998) Role of the C terminus of FtsK in *Escherichia coli* chromosome segregation. *J Bacteriol* **180**: 6424–6428
- Zhou JM, Boyer PD (1993) Evidence that energization of the chloroplast ATP synthase favors ATP formation at the tight binding catalytic site and increases the affinity for ADP at another catalytic site. *J Biol Chem* **268**: 1531–1538

## Conflict of interest

The authors declare that they have no conflict of interest.

 The EMBO Journal is published by Nature Publishing Group on behalf of European Molecular Biology Organization. This article is licensed under a Creative Commons Attribution-NonCommercial-Share Alike 3.0 Licence. [<http://creativecommons.org/licenses/by-nc-sa/3.0/>]